Vol.(4),No.(2),(2016),1-10
MUTHANNA JOURNAL OF ENGINEERING AND TECHNOLOGY (MJET)
مجلة المثنى للهندسة والتكنولوجيا
Journal homepage:www.muthjet.com
Print ISSN:2572-0317, Online ISSN:2572-0325

Shear Behavior of Slender Ferro cement Box Beams

Aqeel H. Chkheiwer[a]*, Mazin A. Al-Mazini[b] , Mustafa Sh. Zewair[c]
Civil Engineering Department, Engineering College, University of Basrah .

ARTICLE INFO

Received: 10/5/2016

Accepted: 21/9/2016

Keywords
Box Beam, Ferrocement, Shear Behavior.

ABSTRACT
This study investigated (experimentally and analytically) the influence of mortar compressive strength (37.4, 48.3 and 60.1 MPa) and the number of wire mish layer in web and bottom flange on the shear behavior of ferrocement slender box beams. To achieve these targets, 12 ferrocement box beams with shear span to effective depth ratio(a/d) of 2.8 (slender beams) are equipped, tested and assessed, all beams having cross section of 300*175 mm, length of 2000 mm and hollow core of 180*115 mm. The tested beams were divided into four groups, each group consists of three beams depending on compressive strength value, the first group was without wire mish, the second group was with one layer of wire mish in web and bottom flange, the third group was two layers of wire mish in web and one in bottom flange and the fourth group was with two layers of wire mish in web and bottom flange. As well as ANSYS-11 program was used to analyze these beams by nonlinear finite element method. Test results showed that, the first cracking and ultimate loads increases as the wire mish layers in web and bottom flange increases, the deflection of the tested beams decreases with increasing mortar compressive strength and wire mish layers in web and bottom flange, the finite element model gives good agreement with the experimental results within 9%.

تصرف القص للأعتاب الفيروسمنتية الصندوقية النحيفة

الخلاصة
تناولت الدراسة (عمليا وتحليليا) تاثيرمقاومة الانضغاط المختلفة(37.4 و48.3 و60.1 نت/ملم^2) للملاط الاسمنتي و عدد طبقات شبكة التسليح في لوح القص والشفه السفلى على سلوك القص للاعتاب الفيروسمنتية الصندوقية النحيفة. لتحقيق هذة الاهداف،تم اعداد وفحص 12 عتبة صندوقية من الفيروسمنت ذات نسبة فضاء القص إلى العمق الفعال 2.8 . حيث كانت كل الاعتاب ذات مقطع عرض بابعاد 300*175 ملم و قلب مجوف بابعاد مقدارها 180*115 ملم وطول 2000 ملم . قسمت العتبات المفحوصة إلى اربع مجاميع وكل مجموعة تتكون من ثلاث عتبات اعتمادا على قيم مقاومة الانضغاط للملاط الاسمنتي.المجموعة الاولى كانت خالية من شبكة التسليح اما المجموعة الثانية كانت تحتوي على طبقة واحدة في لوح القص والشفة السفلى، بينما المجموعة الثالثة احتوت على طبقتين في لوح القص وطبقة واحدة في الشفة السفلى و الرابعة احتوت على طبقتين في لوح القص والشفة السفلى.اضافة إلى ذلك تم استخدام طريقة العناصر المحددة (برنامج **ANSYS-11**) لتحليل العتبات المفحوصة. اظهرت النتائج ان حمل التشقق الاول والحمل الاقصى يزداد بزيادة عدد طبقات شبكة التسليح في لوح القص والشفة السفلى للعتبة. بينما تبين ان اود العتبات يقل بزيادة مقاومة الانضغاط وعدد طبقات شبكة التسليح في لوح القص والشفة السفلى.أعطت نتائج التحليل اللاخطي للعتبات بطريقة العناصر المحددة توافق جيد مع النتائج العملية في حدود 9%.

الكلمات المفتاحية
العتبات الصندوقية، الفيروسمنت، تصرف القص.

*Corresponding author.
E-mail addresses: aqeelcivil@yahoo.com

DOI: 10.18081/mjet/2016-4/1-10

Introduction

Ferrocement (FC) is defined as wire mesh reinforcement impregnated with mortar to produce elements of small thickness, high durability and resilience and, when properly shaped, high strength and rigidity.

The ferrocement is recommended to be used for curves and folded thin elements with a rigidity due to the form and not to the quantity of the material. Due to thin wall construction, ferrocement structures can be made relatively light and water tight [1].

The behavior of ferrocement in flexure has been observed to be very similar to that of reinforced concrete members [2]. However, it has been found that a ferrocement beam acts more like a steel member than reinforced concrete under flexure, and hence ferrocement is considered as a hybrid material between reinforced concrete (material exhibiting cracking etc.) and steel (an elasto-plastic material with large ductility and resilience).

Mansur and Ong (1987) [3] have investigated the behavior in shear of solid ferrocement beams by conducing flexural tests on rectangular beams. It was found that the diagonal cracking strength increases as the shear span to beam depth ratio a/h is decreased and the volume fraction of reinforcement, mortar strength, and the moment of reinforcement near the compression face are increased.

Abdul Samad et al (1998) [5] investigated the structural behavior of the ferrocement box beams subjected to two point load tests which induce pure bending moment with shear force. It was found that, with lower shear span to effective depth (a/d) ratio ($\leq$ 1) ,the more prominent mode failure was the diagonal tension failure, for the higher value of a/d (>1) tends to develop flexural failure of the beam. The ferrocement box section beams had very high shear capacity with very low a/d ratio (0.7).

Rao et al (2006)[4] conducted tests on ferrocement beams varying the shear span to effective depth ratio (a/d) and different layers of mesh are conducted. It was observed that increase in the volume fraction of the mesh reinforcement (number of layers of mesh) increased the shear capacity of the member. It is also found that up to shear span to effective depth ratio 3, shear behavior is predominant. Beyond shear span to depth ratio 3, the flexural behavior is predominant and design of the elements based on flexure is sufficient.

Limited researches are available on the shear strength of slender ferrocement box beams, as the cross section of these beams is hollow. However, studies on the shear behavior of ferrocement assume important to understand the material response .In this study, the effect of compressive strength of mortar, wire mish reinforcement layers in web and bottom flange on the shear behavior of fibrocement slender box beams was investigated. Also the load-deflection curve and crack patterns of the tested beams were monitored at all stages of loading. The finite element modeling and analysis for the beams were conducted to examine the accuracy of finite element method for present the experiment cases.

Experimental Program

The behavior of ferrocement box slender beams falling in shear was investigated in this study. The studied parameters included amounts of wire mesh reinforcement in webs and bottom flange, and compressive strength of mortar. The tested beams were divided into four groups according to the amount of wire mesh reinforcement in webs and flange, with f'c (compressive strength) of 37.4, 48.3 and 60.1 MPa for each group. Table (1) describes the four groups, each group includes three beams. All beams were hollow section with same cross-section 300*175 mm, web thickness of 30 mm and thickness of top and bottom flange of 60 mm. All box beams have same length of 2000 mm to obtain shear span to effective depth ratio (a/d) of 2.8, as shown in Fig. (1). The beam notation consists letter and numbers, the letter B indicates to type of member (Beam),the first, second and third numbers represents water to cement ratio of mix of beam(3 indicates to W/C=0.3) ,number of wire mish layer in bottom flange and number of wire mish layer in web respectively as illustrated in Table (1) .

Expanded metal mesh of 8.4 mm square opening, 1 mm wire diameter and 314 MPa average yield strength was used for beams in groups 2,3 and 4, as seen in Fig.(2). The amounts of wire mesh reinforcement were varied by varying the number of layers of wire mesh in each web (0, 1 and 2) and in bottom flange (0, 1 and 2). Each beam reinforced with four 12 mm diameter bars with yield strength of 450 MPa in the bottom flange to increase its flexural capacity so that shear failure was the dominating mode of failure. It should be noted that the contribution of these regular bars to shear resistance of ferrocement through dowel action was neglected here.

The mortar materials used were cement, fine aggregate (sand), water and superplasticizer. The cement used was Ordinary Portland cement with specific gravity of 3.15 and Blaine fineness 3100cm^2/g, Table (2) presents the Physical properties and chemical composition of this cement. The fine aggregate used was local natural fine sand from Zubair zone in Basrah city, with fineness modulus of 1.51. The fine aggregate had specific gravity of 2.65 and water absorption of 1.30 %. High efficiency superplasticizer (Flowcrete PS 90) as per ASTM C494 – type G [7] having a specific gravity of 1.08 and a total solid content of 38 % was used. Ordinary tap water is used for mixing and curing.

The cement to sand ratio was 1: 2.2 by weight for all mixes. Water/ cement ratio were 0.3, 0.4 and 0.5. The superplasticizer dosages were selected to give flowing mortar (to not need for mechanical compaction). For each mix, three 100 mm cubes

were cast to determine the compressive strength (f_{cu}) of the mortar and three cylinders (150*300 mm) were cast to measure the splitting tensile strength. Table (3) presents mix proportions and properties of mortar used in this study.

Table (1) Test program

Group	Beam No.	Compressive strength (MPa)	W/C ratio	Wire mesh layers in	
				bottom flange	web
1	B003	60.1	0.3	0	0
	B004	48.3	0.4	0	0
	B005	37.4	0.5	0	0
2	B113	60.1	0.3	1	1
	B114	48.3	0.4	1	1
	B115	37.4	0.5	1	1
3	B123	60.1	0.3	1	2
	B124	48.3	0.4	1	2
	B125	37.4	0.5	1	2
4	B223	60.1	0.3	2	2
	B224	48.3	0.4	2	2
	B225	37.4	0.5	2	2

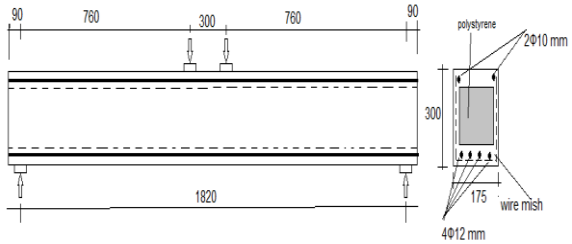

Figure 1. Details of the tested beams (all dimensions in mm)

Table 2. Physical properties and chemical composition of cement

Physical properties		Limits of I.O.S No.45-1984[6]
Setting time (min)		
Initial	120	> 45
Final	245	< 600
Compressive strength (MPa)		
7 days	18.9	> 15
28 days	26.4	> 23
Specific surface, blaine,cm^2/g	3100	> 2300
Chemical analysis,%		
Lime (CaO)	61.89	
Silica (SiO_2)	21.23	
Alumina (Al_2O_3)	5.50	
Iron Oxide (Fe_2O_3)	2.99	
Magnesia (MgO)	2.64	< 5
Sulfate (SO_3)	2.01	2.8
Loss on Ignition (LOI)	0.75	< 4
Insoluble residue (I.R.)	0.60	< 1.5
Lime saturation factor (L.S.F)	0.84	0.66-1.02

The mould is well oiled before placing the steel and wire mish frame with polystyrene cores of the same size as that of the hollow portion (i.e. 2000 mm x 180 mm x115 mm)as seen in Fig.(2).After fixing this frame in mould in suitable location (to avoid polystyrene buoyancy), the self flowing mortar was poured in the mould carefully until filling to the top surface of the mould. The moulds were removed after 3 days of casting and the specimens were moist cured for seven days and then still in libratory conditions until age of testing (28 days). The cubes and cylinders (to determine compressive strength and splitting tensile strength, respectively) were prepared under the same conditions of casting and curing of corresponded beams.

Table 3. Mixture Proportions and properties of mortar

Water cement ratio		0.3	0.4	0.5
Mixture Proportions	Unit			
Water	kg/m^3	198	256	310
Cement	kg/m^3	660	640	620
Sand	kg/m^3	1452	1408	1364
Superplasticizer	L/m^3	11.0	7.8	2.0
Hardened mortar properties				
Cube ompressive strength (f_{cu})	MPa	60.1	48.3	37.1
Splitting tensile strength	MPa	**4.55**	3.67	2.91

Figure 2. Beam casting

The beams were simply supported and tested in flexure two symmetrical point load (see Fig.(1). For this purpose, a universal testing machine with a 100 ton capacity was used. Deflection at midspan was measured by using dial gage with accuracy 0.01 mm per division. During testing, the initiation of crack pattern of each beam at the end of testing was noted to help to assess the failure pattern.

Figure 3.Test set-up

Test Results and Discussion

1. General behaviors under loading

The general behavior (crack development and failure mechanism) of ferrocement beams was quite similar. First, the flexural cracks initiated in the pure bending region. With further increase of load new flexural cracks formed in the shear spans and curved toward the loading points. The failure in the specimens without wire mish was sudden and in diagonal tension shortly after diagonal shear cracks appeared. It is noticed that the ultimate shear capacity of these beam elements was only slightly higher than the load which caused diagonal cracking unlike the failure of the beams with wire mish, where the failure delayed on the emergence of diagonal crack. It is observed that all beams show almost the same crack pattern and failure mechanism, where all beams failed due to diagonal tension shear.

2. Cracking and Ultimate Load

The first flexural cracking (P_{cr}) and ultimate shear loads (P_u) are presented in Table (4).From this table it can be observed that, the first flexural cracking load increases with the increase in cube compressive strength (f_{cu}) of mortar for all tested beams, where in group one, the first cracking load of beams with fc of 48.3 and 60.1 MPa was higher than that of beam having f_{cu} of 37.4 MPa by 10.7 % and 24.3 % respectively. This is attributed to that the tension strength of concrete increases with increasing the compressive strength as illustrated in Table (3).

It can be seen from Table (4), the addition of wire mish with one layer in web and bottom flange (group No.2) leaded to increase P_{cr} by about 7.6% higher than group No. 1. The first crack load of group No.3 and No. 4 beams increased 9.8 % and 10.8% compared with that of group No.1. The wire mish founded in a bottom flange had more effect on the first flexural cracking load than that in a web. This is attributed to that the presence of wire mish in the mortar mixture increases the stiffness of beam as result of increase of the second moment area of beam section.

Table (4) Test results of the tested beams

Group No.	Beam notation	f_{cu} (MPa)	Cracking load, P_{cr} (kN)	Ultimate load, P_u (kN)	P_{cr}/P_u ratio %	Average of P_{cr}/P_u ratio %
1	B003	60.1	25.10	65.30	38.44	37.12
	B004	48.3	22.37	60.50	36.98	
	B005	37.4	20.20	56.20	35.94	
2	B113	60.1	27.85	97.30	28.62	26.82
	B114	48.3	23.56	91.30	25.80	
	B115	37.4	21.50	82.50	26.06	
3	B123	60.1	28.12	131.20	21.43	21.66
	B124	48.3	24.60	112.30	21.91	
	B125	37.4	21.71	100.30	21.65	
4	B223	60.1	28.50	136.90	20.82	19.94
	B224	48.3	24.89	128.70	19.34	
	B225	37.4	21.75	110.80	19.63	

From Table (4) it can be noted that, the ultimate load increased with the increase in compressive strength of mortar (f_{cu}) for all tested beams, where in group No.1, the beams with f_{cu} of 48.3 and 60.1 MPa showed ultimate load 7.6 and 16.2 % higher compared with beam having f_{cu} of 37.4 MPa. This is attributed to same previous reasons in first crack load. It can be observed from Table (4) that , the addition of wire mish exhibited apparent effect on the ultimate shear load ,where in group No.2 , P_u increased by about 48.9 % higher than group No. 1.the ultimate load of group No.3 and No.

4 beams increased by 88.3 % and 106.2 % compared with that of Group No.1 beams .

Table (4) shows also the cracking to ultimate load ratios of all beams in the four groups. It can be clearly seen that, this ratio decreased as the number of wire mish layers increased. That means that, with increase of the wire mish layers, the revised beam strength after appearing the first crack increases. This due to that, a wire mish avoids the tension cracks expansion suddenly; this gives the beam a wide range to distribute the stresses through its elements.

3. Load-deflection curve

Fig.(4) presents load- mid span deflection curves of all tested beams at different loading stages. It can be observed that, the deflection of beams decrease with increase of concrete compressive strength. This is attributed to that modulus of elasticity increases as a compressive strength increases. With the same applied load, the deflection decreased with increasing f_{cu}, this is because that deflection is influenced by the beam stiffness.

On overall, By increasing wire mish layers in web and flange, the deflection values of the beams decreased at same as shown in Fig(4). This is attributed to that reducing the wire mish steel area will reduce the second moment of area of the section. However, the effect of increase wire mish in flange on the deflection value was higher than that of web.

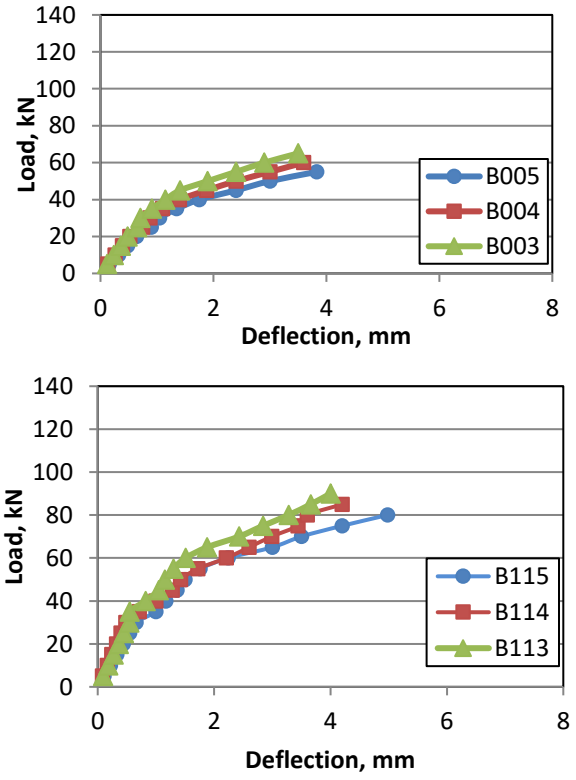

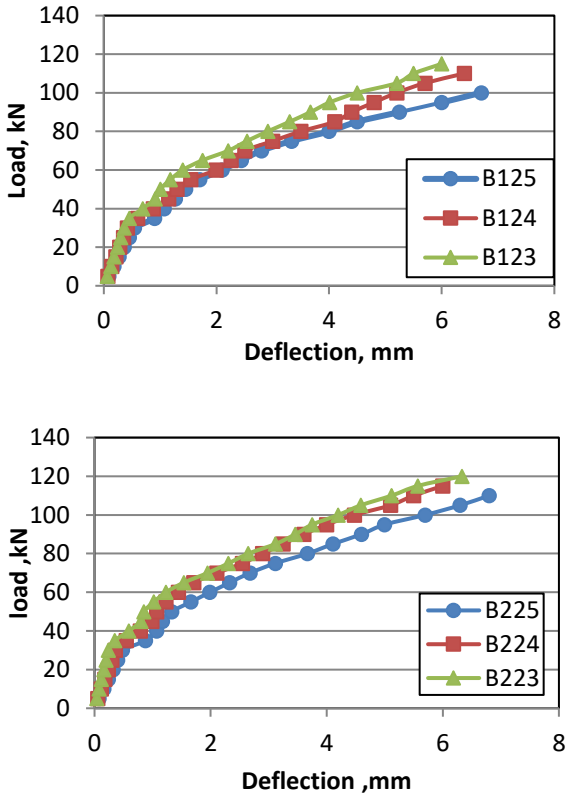

Figure 4. Load- deflection curve of all tested beams

4. Crack patterns

The crack patterns for all tested specimens are shown in Figs. (5) to (8). For all tested beams, the first cracks were vertical cracks (flexural cracks) at mid span region. The diagonal cracking load was close to the failure load for beams without wire mish, the diagonal crack that causing failure started suddenly from the last flexural crack that became inclined and crossed mid depth in shrar span region, and then such a crack propagated simultaneously towards the load-point and towards the support along the tensile reinforcement (due to dowel action) causing a loss of bond and failure of the beam. For beams with wire mish, the failure delayed than the appearance of diagonal crack depending on the number of layers used. From figs.(5) to (8) it can be observed that, the number of narrow diagonal cracks in shear span increased as web wire mish layers increases.

Figure 5. Crack pattern of group one ferrocement beams

Figure 6. Crack pattern of group two ferrocement beams

Figure 7. Crack pattern of group three ferrocement beams

Figure 8. Crack pattern of group four ferrocement beams

4. Finite element modeling

As part of the research, a total of twelve FE models are established and the numerical solutions are correlated with the experimental results. The FE models are created using the finite element (FE) code ANSYS-11[8]. The models have the same geometry, dimensions, and boundary conditions of the tested concrete hollow section beam specimen.

By taking advantage of the symmetry of the beams, a half of the full beam was used for modeling. This approach reduced computational time and computer disk space requirements significantly. Half of the entire model is shown in Fig. (9).

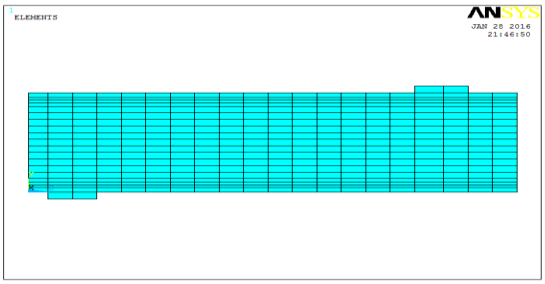

Figure 9. **Typical half symmetry finite element model**

For modeling RC beam, eight nodes Solid65 element with three degrees of freedom at each node (translations in the nodal x, y, and z directions), which handles nonlinear behavior, cracking in three orthogonal directions due to tension, crushing in compression and plastic deformation is used. For modeling reinforcement, two nodded Link8 spar element with three degrees of freedom at each node (translations in the nodal x, y, and z directions), which handles plasticity, creep, swelling, stress stiffening and large deflection is used. In order to avoid stress concentration problem, the supports and loading points are modeled with eight nodded Solid45 element with three degrees of freedom at each node (translations in the nodal x, y, and z directions), which handles plasticity, creep, swelling, stress stiffening, large deflection and strain.

5. Comparison of Experimental and Finite Element Results

Table (5) compares the ultimate loads for the full-size beams and the final loads from the finite element simulations. In general, the predicted ultimate load obtained by ANSYS gives a good agreement with experimental result. For the most part beams, the finite element ultimate load were overestimates than the experimental results by (5%-11%) respectively. ANSYS underestimates the strength of the other beams by (2%-12%). One reason for the discrepancy is that Toughening mechanisms at the crack faces may also slightly extend the failures of the experimental beams before complete collapse. The finite element models do not have such mechanisms.

The experimental load–deflection responses for the tested beams are plotted with the finite element results in Figs. (10) to (13). In general, the load–deflection plots for all beams from the finite element analyses agree quite well with the experimental data. The finite element load–deflection curve is slightly different from the experimental curve. There are several effects that may cause this situation. First of all, microcracks are present in the concrete for the tested beam and could be produced by drying shrinkage in the concrete and/or handling of the beam. On the other hand, the finite element models do not include the microcracks. The other is that perfect bond between

the concrete and reinforcing steel is assumed in the finite element analysis, but the assumption would not be true for the tested beam. In ANSYS, stresses and strains are calculated at the integration points of the concrete solid elements.

Table 5. Comparison between experimental and numerical analysis

Beam	Num. Crack load (kN)	Num. failure load (kN)	Exp. failure load (kN)	$\frac{P_{failure}(Num.)}{P_{failure}(Exp.)}$
B003	24.8	64.6	65.3	0.99
B004	22.1	63.5	60.5	1.05
B005	19.0	53.4	56.2	0.95
B113	27.3	95.4	97.3	0.98
B114	23.4	92.2	91.3	1.01
B115	20.4	77.6	82.5	0.94
B123	26.8	133.8	131.2	1.02
B124	23.1	107.8	112.3	0.96
B125	20.6	90.3	100.3	0.90
B223	27.9	127.3	136.9	0.93
B224	22.6	117.1	128.7	0.91
B225	20.4	104.2	110.8	0.94

A plot of the state of the concrete for the last load step is shown in Fig. (14). In the crack pattern, obtained from the FE model, several flexural cracks can be noted, together with the splitting in the tension zone. The critical diagonal tension crack can also be observed in the shear span zone, between the load point and support, see Fig. (14). The crack pattern in Fig. (14) illustrates an interpretation of the vector crack normal, according to the FE-analysis. These FE crack patterns were almost similar to experimental crack patterns. The horizontal crack along tension reinforcement did not apparent in FE model this is attributed to that this crack is a result of diagonal tension shear failure.

ANSYS displays circles at locations of cracking or crushing in concrete elements. Cracking is shown with a circle outline in the plane of the crack, and crushing is shown with an octahedron outline. If the crack has opened and then closed, the circle outline will have an X through it. Each integration point can crack in up to three different planes. The first crack at an integration point is shown with a red circle outline, the second crack with a green outline, and the third crack with a blue outline.

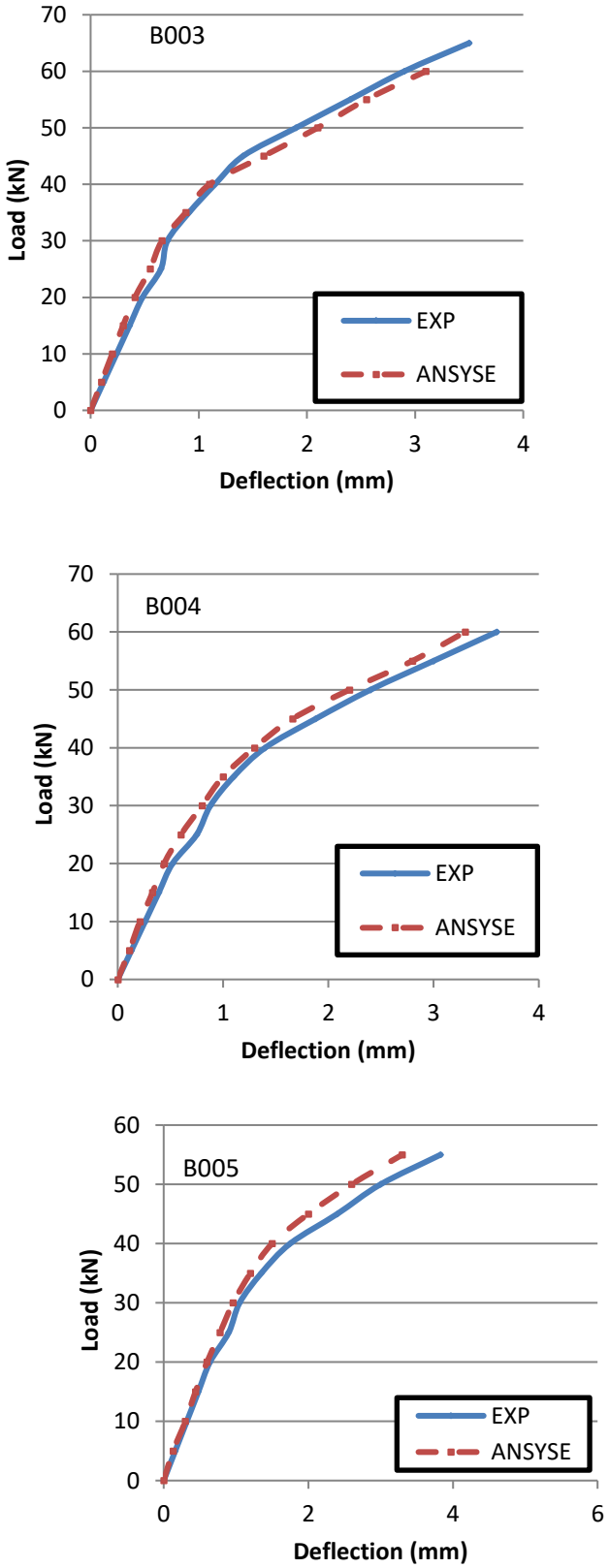

Figure 10. Experimental and theoretical load- deflection curve of group one beams

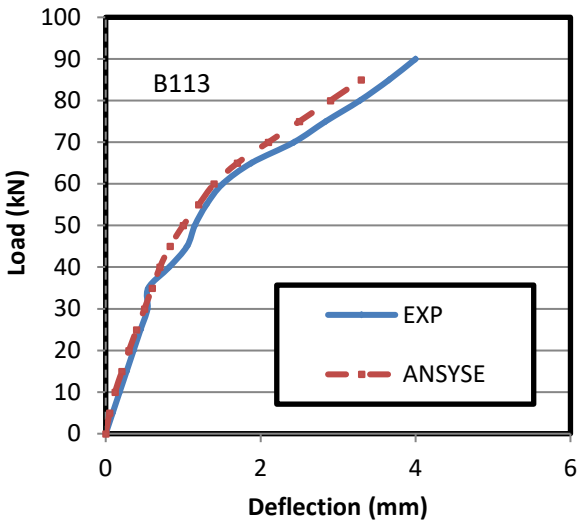

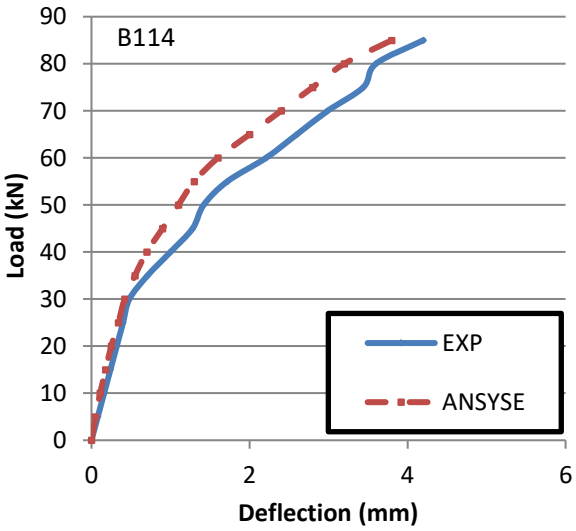

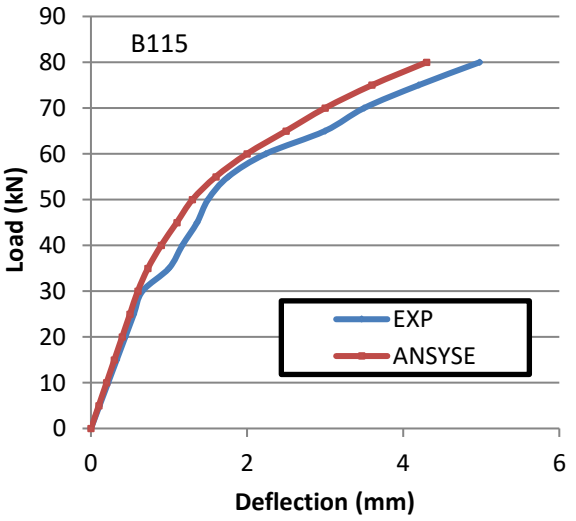

Figure 11. Experimental and theoretical load-deflection curve of group two beams

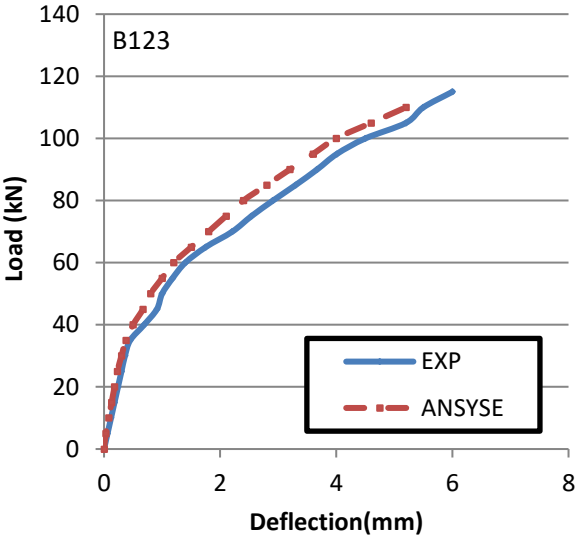

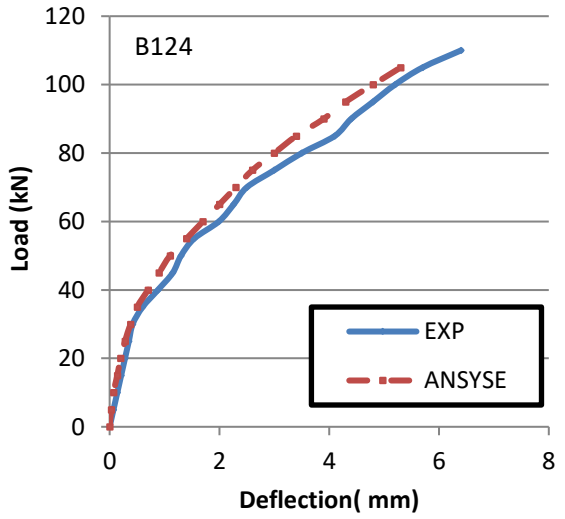

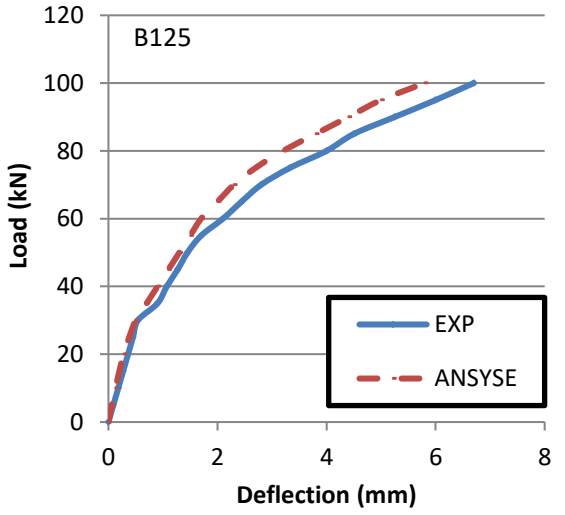

Figure 12. Experimental and theoretical load-deflection curve of group three beams

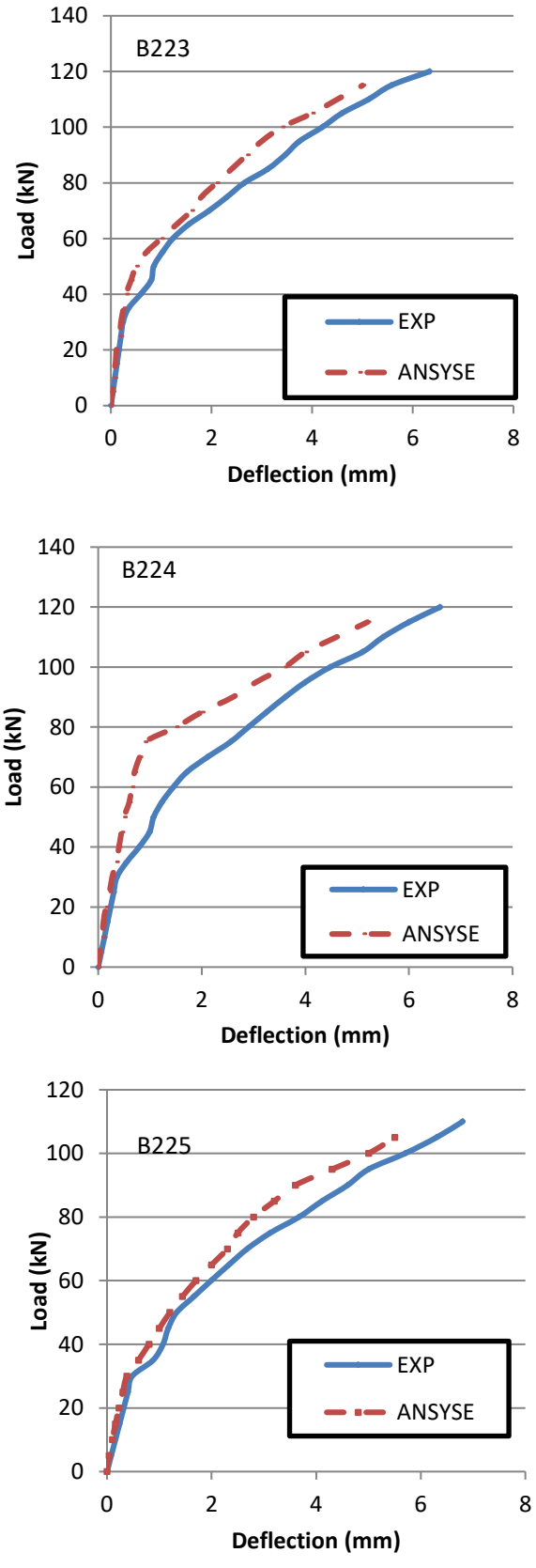

Figure 13. Experimental and theoretical load-deflection curve of group four beams

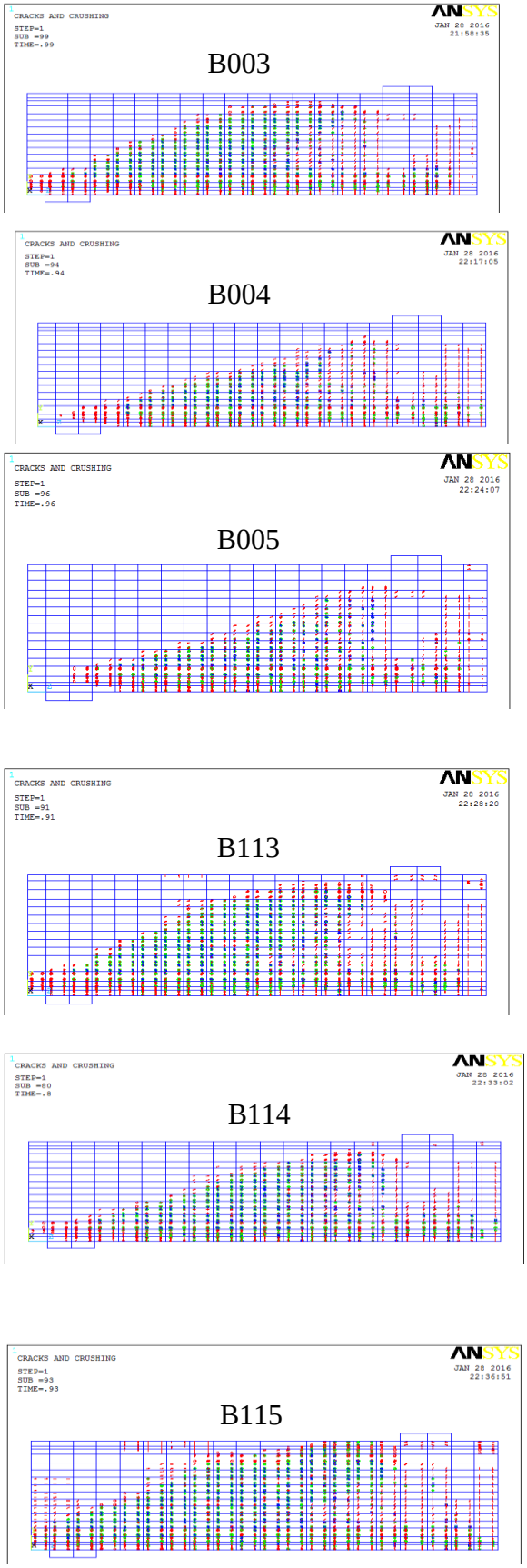

Figure 14. Typical crack patterns of FE model

Conclusions

From this study the following conclusions can be drawn:

1- The first flexural cracking load of beams with mortar compressive strength of 48.3 and 60.1 MPa was higher than that of beam having mortar compressive strength of 37.4 MPa by 10.7% and 24.3% respectively.
2- The beams with mortar compressive strength(f_{cu}) of 48.3 and 60.1 MPa showed ultimate load 7.6% and 16.2% higher compared with beam having f_{cu} of 37.4 MPa respectively.
3- The first cracking and ultimate load increases as the wire mish layers in web and bottom flange increases.
4- First crack to ultimate load ratios reduces with increasing wire mish reinforcement of web and bottom flange.
5- At the same load, the deflection of the tested beams decreases with increasing compressive strength and wire mish layers in web and bottom flange.
6- The number of narrow cracks increases with the increases of wire mish reinforcement
7- The finite element model gives good agreement with the experimental results(first crack load, ultimate load , load deflection curves, and crack pattern)

References

1- Anwar A.W. 1993 “Ferrocement for Low-Coast Housing in Pakistan”, Journal of Ferrocement, 23(2), pp. 117-123.
2- Logan, D. and Shah, S.P., 1973 “Moment Capacity and Cracking Behavior of Ferrocement in Flexure”, ACI Journal Proceeding, 70(12), Dec., pp.799-804.
3- Mansur, M.A. and Ong K.C.G., 1987 “Shear Strength of Ferrocement Beams”. American Concrete Institute Structural Journal, 84(1), pp.10-17.
4- Abdul Samad, A.A., Rashid M.A., Megat Johari, M.M.N. and Abang Abdulla A.A 1998 “Ferrocement box beams subjected to pure bending and bending with shear”. Journal of Ferrocement, 28,.
5- Rao T.C., Rao T.D.G. and Rao N.V.R., 2006 “An Appraisal of the Shear Resistance of Ferrocement Elements”, Asian Journal of Civil Engineering (Building and Housing), Vol.7, No.6,.
6- Iraqi Standards, 2004 “Ordinary Portland cement”, Ministry of Housing and Construction, Baghdad, No.5/1984.
7- ASTM C494-04, 2004 “Standard Specification for Chemical Admixtures for Concrete”, Vol. 4.2, , pp. 1-9.
8- ANSYS, 2006” ANSYS Help”, Release 11.0, USA, copyright, Edition, John Wiley and Sons, New York, 1981.